ELSEVIER

Advances in Water Resources 25 (2002) 477–495

Advances in Water Resources

www.elsevier.com/locate/advwatres

Review

Considerations for modeling bacterial-induced changes in hydraulic properties of variably saturated porous media

M.L. Rockhold [a,b,*], R.R. Yarwood [a], M.R. Niemet [c], P.J. Bottomley [d], J.S. Selker [a,*]

[a] *Department of Bioengineering, Gilmore Hall, Oregon State University, Corvallis, OR 97331, USA*
[b] *Pacific Northwest National Laboratory, Box 999, Richland, WA 99352, USA*
[c] *CH2M Hill, 2300 NW Walnut Blvd., Corvallis, OR 97330, USA*
[d] *Department of Microbiology, Nash Hall, Oregon State University, Corvallis, OR 97331, USA*

Received 28 June 2001; received in revised form 20 December 2001; accepted 29 December 2001

Abstract

Bacterial-induced changes in the hydraulic properties of porous media are important in a variety of disciplines. Most of the previous research on this topic has focused on liquid-saturated porous media systems that are representative of aquifer sediments. Unsaturated or variably saturated systems such as soils require additional considerations that have not been fully addressed in the literature. This paper reviews some of the earlier studies on bacterial-induced changes in the hydraulic properties of saturated porous media, and discusses characteristics of unsaturated or variably saturated porous media that may be important to consider when modeling such phenomena in these systems. New data are presented from experiments conducted in sand-packed columns with initially steady unsaturated flow conditions that show significant biomass-induced changes in pressure heads and water contents and permeability reduction during growth of a *Pseudomonas fluorescens* bacterium.

Keywords: Bioremediation; Unsaturated porous media; Surface tension; Fluid-media scaling

Contents

* Corresponding authors. Address: Department of Bioengineering, Gilmore Hall 116 (M.L. Rockhold)/240 (J.S. Selker), Oregon State University, Corvallis, OR 97331, USA. Tel.: +1-541-737-5410 (M.L. Rockhold)/+1-541-737-6304 (J.S. Selker); fax: +1-541-737-2082.
E-mail addresses: rockhold@engr.orst.edu (M.L. Rockhold), selkerj@engr.orst.edu (J.S. Selker).

0309-1708/02/$ - see front matter
PII: S0309-1708(02)00023-4

1. Introduction

Bacterial-induced changes in the hydraulic properties of porous media have been studied for various applications ranging from enhanced oil recovery, to water and wastewater treatment, to bioremediation of contaminated soils and aquifer systems. Biodegradation of anthropogenic contaminants in soils and aquifers involves many complex interactions between physical, chemical, and biological processes. Improved understanding of these processes and interactions is necessary to achieve more effective bioremediation in field applications.

Several conditions are needed for biodegradation and effective bioremediation [3]. One of these is that the environment must be conducive to the proliferation of the microorganisms of interest. Although proliferation of microorganisms is necessary, it can also have detrimental effects. For example, biomass accumulation can result in clogging of pore space and well bore biofouling at nutrient injection wells [44]. This biofouling can restrict or prevent further injection of nutrients, which can reduce the effectiveness of a bioremediation system. In the oil industry, however, selective plugging of pore space has been used to enhance oil recovery during water injection. In situ microbial growth in liquid-saturated systems can selectively plug high permeability zones and tends to drive an initially heterogeneous permeability field toward homogeneity [33,55]. An open question is if microbial growth and accumulation in heterogeneous, unsaturated porous media systems will manifest greater heterogeneity, or if it will have a homogenizing effect as seen in saturated systems.

The objectives of this paper are to review some of the earlier studies on bacterial-induced changes in the hydraulic properties of saturated porous media, and to discuss characteristics of unsaturated or variably saturated porous media that may be important to consider when modeling such phenomena in these systems. Previously published work on conceptual and mathematical models and experimental studies of biomass growth and accumulation in saturated porous media is reviewed to identify some of the issues and progress to date. Characteristics of variably saturated or unsaturated systems are discussed to identify additional processes that may need to be considered for modeling changes in the hydraulic properties of variably saturated porous media. New data from column experiments are presented that show the affects of biomass growth on pressure head and water content distributions in unsaturated sand. Finally, several methods are discussed that can be used for modeling bacterial-induced changes in the hydraulic properties of variably saturated systems. These methods include fluid-media scaling, and a composite media model for hydraulic properties.

2. Liquid-saturated porous media systems

Various conceptual and mathematical models have been developed to describe substrate utilization or contaminant biodegradation and bacterial growth and transport in saturated porous media systems. Three different approaches have been used most often for this type of modeling [6]. These are: (1) the biofilm model, (2) the microcolony model, and (3) the strictly macroscopic model. A biofilm can be loosely defined as the layers of bacterial cells and associated extracellular material that form on a surface. The biofilm modeling approach assumes that the attached biomass forms a continuous biofilm of uniform thickness covering all solid particles [70–73]. The microcolony modeling approach assumes that bacteria attach to soil or aquifer solids in discrete colonies, each with an effective surface area through which substrates diffuse [50,83,84]. The biofilm and microcolony modeling approaches have both been used to explicitly account for possible substrate diffusional limitations through an attached biomass phase. The strictly macroscopic modeling approach assumes that bacteria can attach and grow in the porous media but makes no other assumptions about the spatial structure or geometry of the attached biomass. In this approach it is usually assumed that no diffusional limitations exist in the biomass and that it is fully penetrated by substrate, nutrients, contaminant, etc. It has been shown that with certain assumptions, the biofilm and microcolony models can be reduced to the strictly macroscopic model [6,58,83]. Recent literature suggests that the macroscopic modeling approach is most commonly used [17,44,52].

A number of experimental studies have been conducted to provide data to support the use of the different conceptual and mathematical models described above, and to evaluate the effects of microbial growth and biomass accumulation on the effective porosity and permeability of saturated porous media. Taylor and Jaffe

[70] conducted experiments in water-saturated, sand-packed column reactors using bacteria isolated from primary sewage and activated sludge from a treatment plant. They used methanol as a substrate, at concentrations of 7.2 and 5.6 mg/l, and observed reductions in saturated hydraulic conductivity, K_s, of more than 3 orders of magnitude at the influent ends of their columns as a result of biomass accumulation. The mean particle diameter of the sand used in their experiments was 0.7 mm. Their data suggest an upper limit to the reduction of K_s of about 3.5 orders of magnitude. They hypothesized that this upper limit represents a balance between growth and accumulation of attached biomass, and biomass loss to the water phase resulting from fluid shear. Taylor et al. [73] and Taylor and Jaffe [71] developed models for permeability reduction and changes in dispersivity based on the concept of bacteria forming biofilms that uniformly cover the grains of the porous media.

Vandevivere and Baveye [75,76] showed that an aerobic bacterial strain, *Arthrobacter* AK19, was able to reduce the K_s of saturated sand columns by 3–4 orders of magnitude within one week when grown on glucose concentrations as low as 10 mg/l. They determined that the production of extracellular polymeric substances (EPS) was not necessary to induce severe clogging. They noted that EPS (polysaccharides) were produced and appeared to cause additional reduction in K_s when the carbon to nitrogen (C:N) ratio was high [77], but EPS seemed to be absent from the clogged layers when the C:N ratio was low (<39). The mean particle diameter of the sand used in their experiments was 0.09 mm.

Fig. 1 shows scanning electron microscope (SEM) images of *Arthrobacter* AK19 taken in sand [76]. Vandevivere and Baveye [76] noted that there was no evidence in their SEM photographs of the bacterium forming biofilms that uniformly covered the pore walls. Instead, their experiments indicated that the cells grew in interstitial spaces where they formed large aggregates. They contend that permeability reduction in saturated porous media systems is caused mainly by the accumulation of bacterial aggregates at pore constrictions where they form local plugs that impede water flow [74–76].

The two primary modes of accumulation of attached bacteria that have been conceptualized and observed in saturated systems—continuous biofilm vs. cell aggregates—raises questions as to what mode of accumulation is most prevalent under what conditions, and how to best represent this accumulation in terms of its effect on porosity and permeability reductions. The answers to these questions are problematic, and depend on the type of bacteria and the environmental conditions. No universally applicable model has been developed for saturated porous media systems. Moreover, no attempts have been made to develop a model that is applicable to both saturated and unsaturated systems.

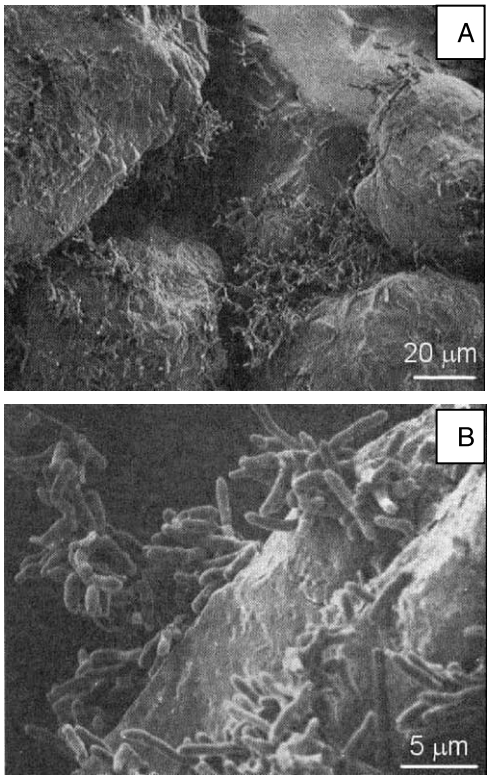

Fig. 1. SEM images of *Arthrobacter* AK19 taken in sand at different magnification (A and B) under conditions of O_2 limitation by Vandevivere and Baveye [75] (with permission).

Rittmann [58] notes that regardless of the characteristics of the attached biomass, net accumulation is controlled by four processes: growth, deposition, decay (or death), and detachment. Growth is generally assumed to be proportional to the rate of substrate utilization and to the amount of biomass already present. Deposition is controlled by the concentration of the aqueous-phase biomass and physicochemical properties of the fluid-media system. Biomass decay is assumed to be proportional to the amount of active biomass. Detachment is generally assumed to be primarily a function of the amount of attached biomass, hydrodynamic shear stress, and growth rate [45,56,69]. Lawrence et al. [36] studied the surface colonization behavior of a *Pseudomonas fluorescens* bacterium and determined that it could be subdivided into the following sequential phases: motile attachment phase, reversible attachment phase, irreversible attachment phase, growth phase, and recolonization phase. These colonization phases may differ between bacterial strains.

Rittmann [58] recognized that different studies have used different types of bacteria, different substrates, different flow rates, and porous media with different mean grain sizes. He attempted to explain and reconcile some of the differences in the characteristics of the attached biomass that have been observed in previous studies by using the concept of normalized surface loading

[30,31,57,82] to standardize results. Normalized surface loading curves can be generated using the biofilm model of Rittmann and McCarty [59,60], which was developed under the assumption that a given biofilm is at steady state and the substrate is completely mixed. Rittmann [58] attempted to establish guidelines for the range of values of normalized surface loading that can be expected to lead to the formation of continuous biofilms versus discontinuous cell aggregates by comparing computed values of normalized surface loading with the observed characteristics of the attached biomass that were reported in previous studies.

Vandevivere [74] developed a model to estimate hydraulic conductivity reduction in saturated porous media systems that incorporates both the uniform biofilm accumulation and cell aggregate clogging mechanisms. He developed the following expression from an analysis of several data sets [18,70,75]

$$\frac{K_s^*}{K_s} = F(B)(1-B)^2 + [1-F(B)]\left(\frac{a}{a+B-aB}\right) \tag{1}$$

where

$$F(B) = \exp\left[-0.5\left(\frac{B}{B_c}\right)^2\right] \tag{2}$$

and where K_s^*/K_s is the ratio of the saturated hydraulic conductivity of the biomass-affected porous medium to the saturated hydraulic conductivity of the "clean" porous medium, $B = 1-(n_b/\phi)$, which is the volume fraction of pore space occupied by bacterial colonies, n_b is the porosity of the biomass-affected porous medium, and ϕ is the original porosity. The parameter a is the value of K_s^*/K_s when the porous medium is completely filled with biomass ($B = 1$), and B_c is an empirical parameter that controls how quickly the system approaches the value of a. The term, $(1-B)^2$ in (1) represents the clogging of a bundle of capillary tubes by continuous biofilms that reduce the effective diameter of the tubes. Vandevivere [74] refers to this as the "biofilm" model. The term, $[a/(a+B-aB)]$, in (1) represents the formation of discrete plugs in some of the tubes in the capillary bundle. Vandeviviere [74] refers to this as the "plug" model. The two terms are combined as a weighted average function of the volume fraction of the total porosity occupied by biomass. Based on the maximum permeability reductions observed in earlier studies, an average value of $a = 0.00025$ was suggested to be adequate for most practical purposes [74]. Alternatively, the a parameter can be determined experimentally. Note that unlike the previous models that have been proposed in the literature, a porous and permeable attached biomass phase is implicitly assumed by the use of non-zero values of the a parameter in (1).

Clement et al. [17] developed analytical expressions for modeling changes in porosity, specific surface area, and permeability caused by biomass accumulation in saturated porous media. Their equations are based on macroscopic estimates of average biomass concentrations and are thus appropriate for use in the macroscopic approaches for modeling substrate utilization. Their results are comparable to the biofilm model results obtained by Taylor et al. [73]. Clement et al. [17] used a cut-and-random-rejoin model of porous media [51,73] and derived the following equations for relative changes in permeability and specific surface area due to biomass accumulation

$$\frac{k_b}{k_0} = \left(1-\frac{n_f}{\phi}\right)^{19/6} \tag{3}$$

$$\frac{M_b}{M_0} = \left(1-\frac{n_f}{\phi}\right)^{2/3} \tag{4}$$

where k_b and k_0 are the permeabilities of the biomass-affected porous medium and the "clean" porous medium, and M_b and M_0 are the specific surface areas of the biomass-affected and clean porous media, respectively. Values of specific surface area were computed by Clement et al. [17] to facilitate comparisons with the biofilm model of Taylor et al. [73]. The volume of sand-associated (attached) biomass/bulk volume of porous media was estimated from

$$n_f = \frac{X_f \rho_b}{\rho_f} \tag{5}$$

where X_f is the mass of microbial cells per unit mass of porous medium, ρ_b is the bulk density of the porous medium, and ρ_f is the density of the microbial cells. Clement et al. [17] calculated the porosity reduction from a simple volume balance

$$n_b = \phi - n_f \tag{6}$$

where n_b is again the porosity of the biomass-affected porous medium. Note that (6) implies that the attached biomass phase is non-porous. With the assumptions used in their derivations, Clement et al. [17] found that Eqs. (3) and (4) resulted from using either the van Genuchten [78] or Brooks and Corey [11] models of water retention, both of which were used to infer the pore-size distributions of the porous media. However, Clement et al. [17] ignored possible changes in the pore-size distribution of the porous media and only accounted for reductions in the maximum pore radius.

Eq. (1) from Vandeviviere [74] is plotted in Fig. 2 with data from Cunningham et al. [18] and Vandevivere and Baveye [75]. Also plotted are the "plug" and "biofilm" models from Vandevivere [74], and Eq. (3) from Clement et al. [17]. Eq. (3) contains no empirical parameters and is essentially equivalent to a biofilm model. The empirical parameter, B_c, in (2) was fit to the data sets depicted in Fig. 2 by Vandevivere [74]. He noted

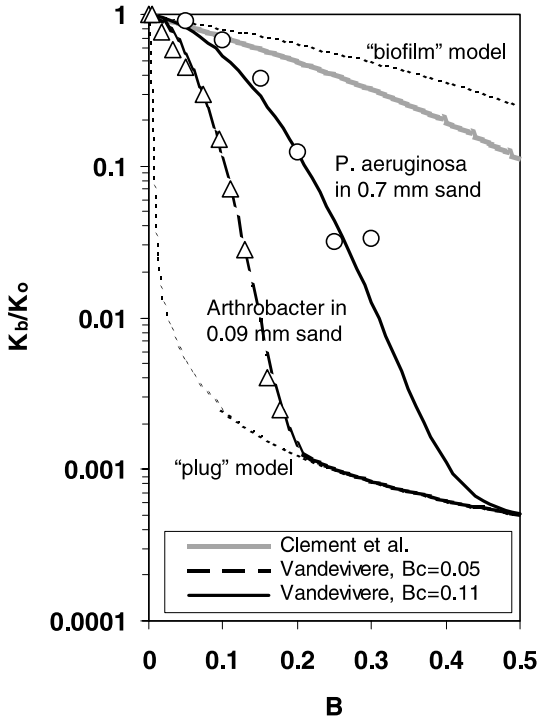

Fig. 2. Models for hydraulic conductivity or permeability reduction in saturated porous media as a function of the volume fraction of pore space occupied by bacterial colonies, *B*. Data for *P. aeruginosa* in 0.7 mm sand is from Cunningham et al. [18], and data for *Arthrobacter* in 0.09 mm sand is from Vandevivere and Baveye [75,76].

that the coarser the texture of the porous media, the greater the fitted value of B_c, and suggested that this observation warranted additional research to obtain independent estimates of B_c for various systems. Vandevivere [74] also noted that any practical use of (1) would require the simultaneous modeling of water flow, transport and utilization of substrate, and biomass growth and accumulation.

Reaching a consensus on a conceptual model for how bacteria attach, accumulate, and alter porosity and permeability in porous media is impeded by the difficulty of observing them in situ under realistic environmental conditions, and by the fact that different bacteria respond to changing environmental conditions differently [13,19,47]. De Beer and Schramm [19] studied the microbial ecology of microenvironments and mass transfer characteristics in biofilms using a combination of microsensor and molecular techniques. They cite earlier work in which confocal microscopy was used to study biofilms and to identify highly complex structures within them. These structures contained layers and clusters of cells, as well as voids or pores [20,21,36]. De Beer et al. [21] determined that the biofilm volumes in their study were up to 50% void spaces. The primary conclusion of De Beer and Schramm [19] was that due to the porous nature of biofilms, convection can be a significant transport mechanism through them. This conclusion is also supported by a number of other recent studies [8,42,43,85].

3. Unsaturated or variably saturated systems

Differences in the behavior of bacteria in unsaturated or variably saturated porous media such as soils, relative to fully water-saturated porous media such as aquifers are due, in part, to the presence of air–water interfaces. Wan et al. [81] showed that preferential sorption of bacteria can occur on air–water interfaces relative to solid–water interfaces. This preferential sorption was shown to be proportional to air saturation. Wan et al. [81] suggest that sorption onto air–water interfaces is controlled primarily by bacterial cell surface hydrophobicity and that this sorption is essentially irreversible. In addition to the hydrophobicity mechanism, preferential growth of aerobic bacteria might also occur at air–water interfaces due to oxygen limitations, especially during high substrate loading conditions. Such limitations could result in oxygen gradients that favor the migration of motile aerobic microorganisms to air–water interfaces via chemotaxis.

The adaptive nature of microorganisms complicates the quantification of their behavior and interactions. This adaptive nature is more apparent in unsaturated or variably saturated porous media systems than in saturated systems due to the additional degree of freedom. For example, Roberson and Firestone [61] and Chenu [15] demonstrated that some bacteria respond to soil drying by increasing the production of EPS which buffers cells from desiccation and also apparently increases the rates of cell attachment to porous media. EPS can also have a tremendous water-holding capacity [15].

Table 1 lists some of the properties of unsaturated or variably saturated porous media systems that may change due to the accumulation of biomass or due to the generation of bi-products of microbial metabolism, such as biosurfactants. These properties include the surface tension at the gas–liquid interface, the solid–liquid contact angle, the bulk solution density and viscosity, and the effective pore structure of the combined porous media/biomass system. The volume and composition of the gas phase may also change as oxygen or other gases are consumed and carbon dioxide or other gases are generated during microbial metabolism [37]. Gas generation and entrapment thus provides an additional mechanism for reducing permeability, in both saturated and unsaturated porous media [14,67]. The processes that we believe are most influential in the alteration of the hydraulic properties of variably saturated porous media, and methods for modeling their changes in flow and transport models, are discussed in more detail in the following sections.

Table 1
Possible effects of biomass accumulation and associated bi-product formation on hydraulic and transport properties of variably saturated porous media

Location of adsorption or accumulation	Possible effects
Gas–liquid interface	Decreased surface tension Increased gas–liquid interfacial area Changes in gas–liquid mass transfer rates
Solid–liquid interface	Decrease in porosity and permeability Changes in apparent contact angle
Liquid–liquid interface (e.g. water–NAPL)	Changes in interfacial tensions Increased solubility of NAPL
Bulk aqueous phase	Increased viscosity Increased solution density Increased solubility of substrates
Cell-to-cell (or particle) aggregation	Physical filtration and pore clogging Decrease in porosity and permeability

3.1. Hydraulic properties of variably saturated porous media

Unlike liquid-saturated porous media systems, unsaturated or variably saturated porous media contain a gas phase which is frequently assumed to be interconnected and at constant, atmospheric pressure. The water content (or saturation) and hydraulic conductivity of variably saturated porous media are non-linear functions of the capillary pressure, rather than being constants as in saturated systems. To aid in this discussion, the equations that relate the capillary pressure to surface tension and other interfacial forces are reviewed.

The pressure difference, Δp, between a gas and liquid phase across their shared interface is related to the curvature of the interface by the well-known Young–Laplace equation

$$\Delta p = p_g - p_l = \sigma_{lg}\left(\frac{1}{R_1} + \frac{1}{R_2}\right) \tag{7}$$

where p_g is the pressure in the gas phase, p_l is the pressure in the liquid phase, σ_{lg} is the surface tension at the liquid–gas interface, and R_1 and R_2 are the principal radii of curvature of the solid surface (e.g. sand grain) and the liquid–gas interfaces, respectively. In capillary tubes and porous media, this pressure difference is usually referred to as the capillary pressure, p_c, which can also be defined as

$$\Delta p \equiv p_c = \frac{2(\sigma_{sg} - \sigma_{ls})}{r} \tag{8}$$

where σ_{sg} is the interfacial tension at the solid–gas interface, σ_{ls} is the interfacial tension at the liquid–solid interface, and r is the effective radius of curvature of a cylindrical capillary tube or spherical pore. The interfacial tensions, σ_{sg} and σ_{ls}, and the effective radius of curvature of the liquid–gas interfaces, R_2 are difficult to measure. Therefore, Eqs. (7) and (8) are usually not used directly, but are expressed in terms of more easily measured variables such as the liquid–gas interfacial tension, σ_{lg}, and an apparent contact angle, γ, between the liquid–gas interface and the solid. Young's equation relates the three interfacial tensions to the apparent contact angle at equilibrium

$$\sigma_{sg} = \sigma_{ls} + \sigma_{lg}\cos\gamma \tag{9}$$

Eqs. (8) and (9) can be combined to yield what is commonly known as the Laplace equation

$$p_c = \frac{2\sigma_{lg}\cos\gamma}{r} \tag{10}$$

When expressed on the basis of an equivalent height of water, Eq. (10) becomes

$$h = \frac{2\sigma_{lg}\cos\gamma}{\Delta\rho g r} \tag{11}$$

where h is the pressure head (negative for unsaturated porous media), which is equivalent to the height to which water would rise in a capillary tube when its lower end is in contact with a free water surface, and $\Delta\rho$ is the density difference between the aqueous and gas phases. The density of the gas phase is usually considered to be negligible relative to the aqueous phase.

Various empirical models have been developed to describe pressure–saturation relations, such as that given by Brooks and Corey [11]

$$\begin{aligned} S_e &= \left(\frac{\theta_w - \theta_r}{\theta_s - \theta_r}\right) = \left(\frac{h_b}{h}\right)^{\lambda} && \text{for } h \geqslant h_b \\ S_e &= 1 && \text{for } h < h_b \end{aligned} \tag{12}$$

where S_e is the effective saturation, θ_r is the residual or irreducible water content, θ_s is the saturated water content or porosity (ϕ), h_b is the air-entry pressure, which is a measure of the maximum pore size forming a continuous network of flow channels through the porous medium, and λ is a pore-size distribution index. The relative permeability, k_r, or hydraulic conductivity, K, of a porous medium can be represented using models such as that given by Burdine [12] or Mualem [51]. When combined with the Brooks–Corey model, the Burdine model can be expressed as

$$k_r = \frac{K}{K_s} = (S_e)^{\varepsilon} \tag{13}$$

or

$$\begin{aligned} k_r &= \left(\frac{h_b}{h}\right)^{\eta} && \text{for } h \geqslant h_b \\ k_r &= 1 && \text{for } h < h_b \end{aligned} \tag{14}$$

where K_s is the hydraulic conductivity of the porous medium when fully saturated with liquid, and where $\varepsilon = 2/\lambda + 3$, and $\eta = 2 + 3\lambda$.

The van Genuchten [78] model is also commonly used to represent the water retention characteristics of variably saturated porous media

$$S_e = \frac{1}{[1 + (\alpha h)^n]^m} \tag{15}$$

where α, n, and m are empirical parameters that affect the shape of the water retention function. Van Genuchten [78] combined (15) with the Mualem [51] hydraulic conductivity model to derive closed-form expressions for the hydraulic conductivity of unsaturated porous media. These expressions for hydraulic conductivity are given by Eqs. (16) and (17),

$$K(S_e) = K_s S_e^{\ell}[1 - (1 - S_e^{1/m})^m]^2 \tag{16}$$

$$K(h) = \frac{K_s\{1 - (\alpha h)^{mn}[1 + (\alpha h)^n]^{-m}\}^2}{[1 + (\alpha h)^n]^{m\ell}} \tag{17}$$

as a function of effective saturation and pressure head, respectively, where ℓ is a pore-interaction term that is often assumed to be equal to 0.5, and $m = 1 - 1/n$ [51,78]. Further discussion on these equations is provided by van Genuchten et al. [79].

Fig. 3 shows the measured water retention characteristics (primary drainage) of a 40/50 grade of quartz sand (Accusand®, Unimin, Co.) measured in our laboratory, a clay soil [38], and xanthan, a pure polysaccharide isolated from the soil bacterium, *Xanthomonas* sp. [15]. Xanthan is widely used in modifying the viscosity of processed foods, in stabilizing suspensions, and in oil field recovery operations [5]. The remarkable water holding capacity of xanthan is clearly evident from Fig. 3. This large water holding capacity has potentially significant implications for the ability of bacteria to modify the hydraulic properties of variably saturated porous media through their production of EPS.

The water retention characteristics of the clean 40/50 Accusand shown in Fig. 3 are plotted with data representing the same sand after a *Pseudomonas fluorescens* HK44 bacterium was allowed to grow in the sand in our laboratory for one week. The sand was originally wet-packed into duplicate, segmented, acrylic columns that were instrumented with tensiometers with pressure transducers, and time-domain reflectometry (TDR) probes, for measurement of pressure heads and apparent volumetric water contents, respectively. The sand was wet-packed into the columns which contained a cell-solution with a concentration of approximately 10^8 CFU/ml (where CFU refers to a colony-forming unit). A steady flux of a minimal mineral salts (MMS) solution containing 250 mg/l glucose was applied to the tops of

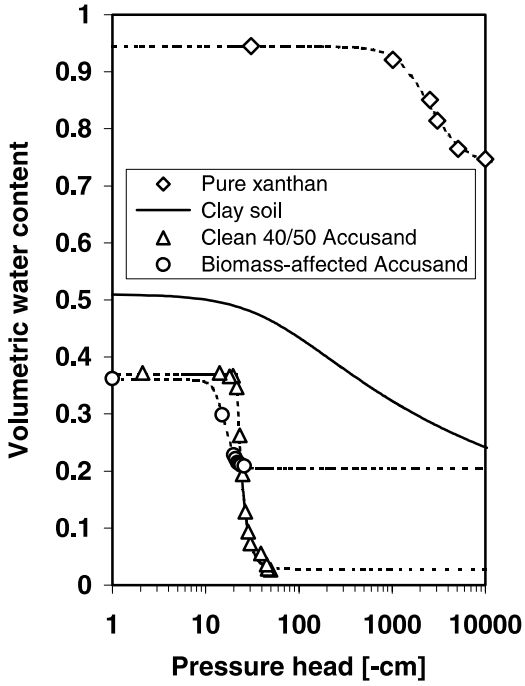

Fig. 3. Water retention data and fitted retention functions for pure xanthan (data from Chenu [15]), a clay soil (model parameters from Leij et al. [38]), clean 40/50 grade Accusand®, and repacked, biomass-affected 40/50 grade Accusand®. The continuous curves represent fits of the Brooks–Corey and van Genuchten water retention models to the data.

the columns at a flow rate of ≈7 cm/h, with the lower boundary maintained at a pressure head of 0 cm. These boundary conditions resulted in unsaturated conditions in the upper halves of the columns with saturated conditions below. Pressure heads and apparent volumetric water contents within the columns were measured during the experiment using the tensiometers and TDR probes, respectively.

After one week, water began to pond on the surface of the columns, indicating that the saturated hydraulic conductivity of the sand at the surface of the columns was reduced from its original value of ≈317 cm/h to less than 7 cm/h. After ponding started, the supply of influent to the tops of the columns was stopped and the upper unsaturated portions of the columns were destructively sampled. Samples were oven-dried at 50 °C for two days to determine gravimetric water contents. The oven-dried, biomass-affected sand formed aggregates which were broken up and passed through a 40 mesh (0.425 mm) screen prior to repacking in Tempe cells (Soil Measurement Systems, Inc.) for water retention measurements. The sand-packed Tempe cells were vacuum saturated prior to initiating water retention measurements. Comparisons of the data representing the clean and biomass-affected sands in Fig. 3 indicates that the biomass had a significant impact on the water retention characteristics of the porous media. The

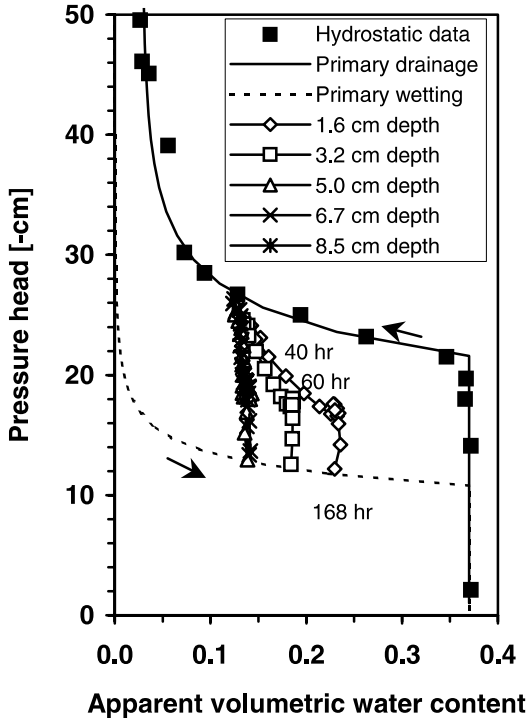

Fig. 4. Water retention characteristics for primary wetting and drainage of clean 40/50 grade Accusand®, and water retention data measured by tensiometry and TDR in columns during growth of a *Pseudomonas fluorescens* HK44 bacterium on glucose under steady flow conditions. Note that the times correspond to times following the introduction of glucose into the columns and the symbols for the transient data represent 10 h increments (except for the final time of 168 h).

wettability of the sand was apparently reduced, but the effective residual water content of the biomass-affected sand was also increased.

Fig. 4 shows the water retention characteristics of the 40/50 Accusand® corresponding to primary drainage and wetting, along with data collected from the tensiometers and TDR probes in our laboratory during the experiment described above. Since steady flow was maintained during the experiment, the changes in pressure head and water content that occurred in the biomass-affected sand depicted in Fig. 4 (transient data) were likely due to changes in contact angle and/or surface tension. Pressure heads increased at all measured depths during the experiment, while increases in the apparent volumetric water content occurred primarily in the upper 3 cm of the columns. Measurements made on sand samples from the columns indicated that little or no EPS was produced under the conditions of the column experiment. The data shown in Fig. 3, however, represent the biomass-affected sand after it was oven dried and repacked. Changes in the water retention characteristics of the biomass-affected sand shown in Fig. 3 are apparently due to changes that occurred during drying. Some of the possible causes for the observed, biomass-induced changes in the hydraulic properties of the sand shown in Figs. 3 and 4 are discussed below.

4. Surface tension effects

Many bacterial cell surface polymers are amphipathic, containing strongly hydrophobic and hydrophilic moieties that tend to concentrate at gas–liquid interfaces [5]. As noted previously, cell hydrophobicity provides a mechanism for sorption of bacterial cells at gas–liquid interfaces. Bacterial cells may also secrete compounds such as polypeptides that can behave like surfactants. Adsorption of bacteria and surfactants at gas–liquid interfaces tends to reduce the interfacial free energy and thus the surface tension. If sorption can be taken to be instantaneous, the Gibbs adsorption equation can potentially be used to relate observed changes in surface tension to the concentration of adsorbed cells and/or surfactants at gas–liquid interfaces [2]. Recent work by Docoslis et al. [24] indicates that the hydrophobic or hydrophilic nature of solutes is also an important consideration when measuring surface tensions of aqueous solutions.

Fig. 5 shows the apparent surface tensions at the gas–liquid interface for different concentrations of stationary-phase *Pseudomonas fluorescens* HK44 suspended in MMS. The surface tensions shown in Fig. 5 were measured using a DuNoüy ring tensiometer (CSC Scientific Co., Inc., Fairfax, VA). Fig. 5 suggests that an approximately linear decrease in surface tension of less

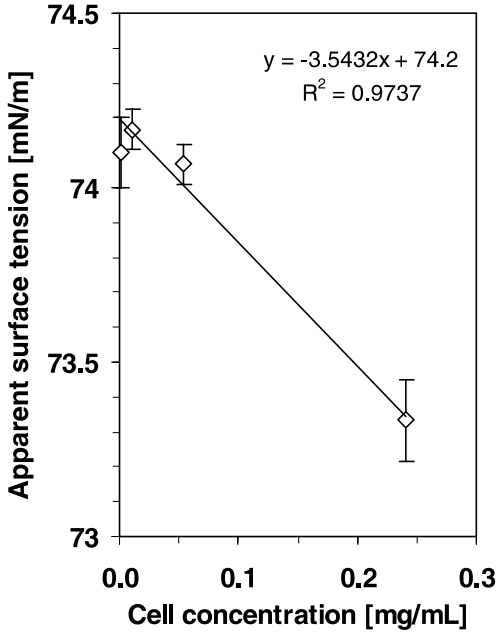

Fig. 5. Apparent surface tension as a function of aqueous phase cell concentrations for the *Pseudomonas fluorescens* HK44 bacterium (error bars represent standard deviation of three measurements).

than 1 mN/m occurs over an almost three-order-of-magnitude increase in cell concentrations ($\sim 10^6$–10^9 CFU/ml) for this particular bacterium in stationary phase. These data suggest that surface tension lowering due to sorption of the cells themselves may be relatively insignificant. However, Déziel et al. [23] conducted a study of a *Pseudomonas aeruginosa* 19SJ bacterium actively growing on the polycyclic aromatic hydrocarbon, naphthalene, and reported a reduction in surface tension from ≈74 to 33 mN/m as a result of biosurfactant production by the bacterium. They did not report the actual cell concentrations that were used in their experiments, but the contrast between their results and the data in Fig. 5 suggest that surface tension lowering effects might be related to the production of surface-active agents during active metabolism. This conclusion is dependent, however, on the type (and metabolic state) of the bacteria, the type of substrate, and on the presence or absence of various trace elements [35].

Déziel et al. [23] determined that the presence of the intermediate metabolite, salicylate, reduced the delay or lag time before accumulation of biosurfactant (glycolipid—rhamnose) in the *P. aeruginosa* 19SJ bacterium. They also determined that the production of biosurfactants in their experiments increased the apparent aqueous solubility of naphthalene by more than a factor of 3 over its normal solubility in water. They suggested that biosurfactant production by bacteria is a self-stimulating process in which the solubilizing effect of biosurfactants increases the availability of insoluble substrates, which in turn promotes further growth and utilization of the substrates. Hammel and Ratledge [28] suggest, however, that surfactant production by microorganisms may be nothing more than a method of removing surplus fatty acids.

In unsaturated porous media, reduced surface tension due to adsorption of cells and/or surfactants at gas–liquid interfaces could lead to lower liquid saturations. Schäfer et al. [64] monitored liquid contents and pressures in unsaturated column experiments during transport of two types of soil bacteria under non-growth conditions. They observed slight increases in liquid saturation during their experiments, but stated that the increase was not caused by a change in surface tension of the liquid in the presence of bacteria. From the previously cited results, and without regard to other factors, the accumulation of biosurfactants would tend to lower surface tension and lead to lower liquid saturation. However, desaturation effects due to surface tension lowering may also be strongly dependent upon the boundary conditions and dimensionality of the experimental system. Local reductions in surface tension and desaturation of a porous medium should result in lower unsaturated hydraulic conductivity, which effectively increases the resistance to flow. This could then lead to increases in upstream saturations, as illustrated in Fig. 4.

5. Contact angle effects

The changes in saturation that are depicted in Fig. 4 could also have resulted, in part, from changes in the apparent contact angle at solid–liquid interfaces as the solids became coated by biofilms. Table 2 lists some physicochemical properties of various bacteria and latex particles, including apparent contact angles (wetting). The contact angle data shown in Table 2 from Wan et al. [81] were measured at the junction of the drop of an aqueous solution, a bacterial surface formed on microporous filter paper, and the atmosphere using a contact angle goniometer. The values reported by Wan et al. [81] represent the means of more than 15 measurements for each bacterium examined. The contact angle in water-wet porous media is generally assumed to be equal to ≈0°, whereas a contact angle of ≈30° can be inferred from data for water imbibition into dry capillary tubes. The data shown in Table 2 clearly indicate that bacteria are capable of altering the wettability of surfaces, and thus changing the water retention characteristics of porous media (see Eq. (11)). Further discussion on contact angle effects is given in a later section on fluid-media scaling.

Decreases in liquid saturation that result from lowering of surface tension and changes in apparent contact angles would also tend to create more gas–liquid interfacial area. Increased gas–liquid interfacial area potentially provides additional sites for cell and biosurfactant adsorption, as well as more surface area for exchange of oxygen and other gases between the aqueous and gas phases. Adsorption of a macromolecular film at the gas–liquid interface can, however, effectively decrease the mass transfer rates of gases across the interface [2,5]. All of these factors may need to be considered for accurate modeling of biodegradation processes in variably saturated porous media.

Bailey and Ollis [5] note that the adsorption of macromolecular films at gas–liquid interfaces can also result in stagnant, rigid interfaces. From a fluid mechanics perspective, the nature of the gas–liquid interface in

Table 2
Selected physicochemical properties of bacteria and colloids

Bacteria or Colloid	Size (μm)	Contact angle, γ_w (deg)	Zeta potential, ζ (mV)
Arthrobacter sp. S-139[a]	1.0×0.8	77.1 ± 2.5	-56.3
P. cepacia 3N3A[a]	1.3×0.8	24.7 ± 3.1	-12.1
Rhodococcus sp. C125[b]	3.0×0.9	95.1 ± 1.7	-44.8 ± 1.4
P. putida mt2[b]	2.2×0.9	38.2 ± 1.5	-13.4 ± 1.0
Latex particles[c]	0.22	127 ± 5	-36

[a] From Wan et al. [81].
[b] From Schäfer et al. [64].
[c] From Wan and Wilson [80].

unsaturated porous media is subject to debate as to whether it more closely resembles a no-slip (e.g. the static wall of a capillary tube) or a slip boundary (e.g. the dynamic gas–liquid interface at the surface of a flowing river), or some combination of the two. Experimental data from Schügerl [66] and Wan et al. [81] provide support for the argument of a limited slip boundary condition.

6. Density and viscosity effects

As cell concentrations increase in the bulk aqueous phase during growth of bacteria, the apparent viscosity and density of the liquid-cell suspension may increase. Several studies have demonstrated the importance of solution density on transport in saturated porous media systems. Istok and Humphrey [32], for example, conducted two-well tracer tests in a homogeneous physical aquifer model and observed significant gravity-induced plume sinking with bromide concentrations as low as 50 mg/l. Murphy et al. [52] determined that accounting for density differences as low as 0.1% was significant for accurately modeling breakthrough of $CaCl_2$ and benzoate in a flow cell containing saturated porous media with bimodal heterogeneities and benzoate-degrading bacteria.

The affects of density differences in unsaturated porous media are usually assumed to be less significant than in saturated porous media because of the lack of buoyancy effects. Ouyang and Zheng [53] conducted numerical experiments to determine the significance of density effects on transport in unsaturated soil. They determined that solution density had a negligible affect on the transport of the chemical aldicarb (relatively low aqueous solubility), but had a significant affect on the transport of the chemical acephate (relatively high aqueous solubility).

Evaluation of the significance of changes in bulk solution density due to bacterial cells is straightforward. Bouwer and Rittmann [9] report that bacterial cell densities range from about 1.01 to 1.13 g/cm^3, with an average value of about 1.1 g/cm^3. If cells are assumed to behave approximately like solid particles, and if the liquid-cell suspension is viewed as a continuum, the average density of a bacterial cell and the volume fraction of cells in suspension can be used to estimate the density and apparent viscosity of the liquid-cell suspension. The density of the liquid-cell suspension, ρ, can be calculated from

$$\rho = \phi_m \rho_m + (1 - \phi_m)\rho_0 \tag{18}$$

where ϕ_m is the volume fraction of cells (or particles) in suspension, and ρ_m and ρ_0 are the densities of the cells and the cell-free liquid, respectively.

Happel and Brenner [29] review various equations that have been used for calculating the apparent viscosity of liquids containing solid particles in suspension. Einstein [25] formula can be used to calculate the apparent viscosity of a dilute suspension of spherical particles

$$\mu = \mu_0 \left(1 + \frac{5}{2}\phi_m\right) \tag{19}$$

where μ_0 is the viscosity of the particle-free suspending liquid. Brodnyan [10] proposed the following equation for the viscosity of concentrated solutions of ellipsoidal particles

$$\mu = \mu_0 \exp\left[\frac{2.5\phi_m + 0.399(p-1)^{1.48}\phi_m}{1 - c\phi_m}\right] \tag{20}$$

where the value 2.5 comes from the Einstein formula (19), the constants 0.399 and 1.48 were determined empirically from experimental data, $p = a_1/a_2$ where a_1 and a_2 are the dimensions of the major and minor axis of the ellipsoidal particle, respectively, and c is an experimentally determined constant that ranges in value from 1.35 to 1.91.

Eqs. (18)–(20) are plotted in Fig. 6, using values of $p = 4.0$ and 1.0, and $c = 1.68$ for Eq. (20). With an average cell density of 1.1 g/cm^3, changes in the density of the liquid-cell suspension are relatively small, increasing by only 1% for a 10% increase in the volume fraction of cells in suspension. Fig. 6 indicates that the potential for changes in the apparent relative viscosity are much more significant than changes in density, especially for ellipsoidal particles. A value of $p = 1$ in the Brodnyan [10] model (20) corresponds to spherical particles, and yields values that are similar to Einstein's results from (19). The differences between the apparent relative viscosities predicted by (19) and (20) are substantial, however, when $p = 4$. This value of p corresponds to ellipsoidal particles whose major axes are four times larger than their minor axes, which is within the range of possible dimensions for rod-shaped bacteria.

In many natural environments, low nutrient availability will limit bacterial cell growth and population densities so that changes in solution density and viscosity due to the accumulation of cells will be relatively small and probably negligible. However, under high nutrient loading conditions, such as might occur in a bioremediation scenario, these changes may be significant.

Murphy et al. [52] noted that physical heterogeneities tend to amplify density and viscosity differences in saturated porous media systems. Furthermore, they noted that macroscopic continuum models of flow and transport may be taxed beyond their theoretical capability when density and viscosity effects are significant because these effects may be due to microscopic pore-scale in-

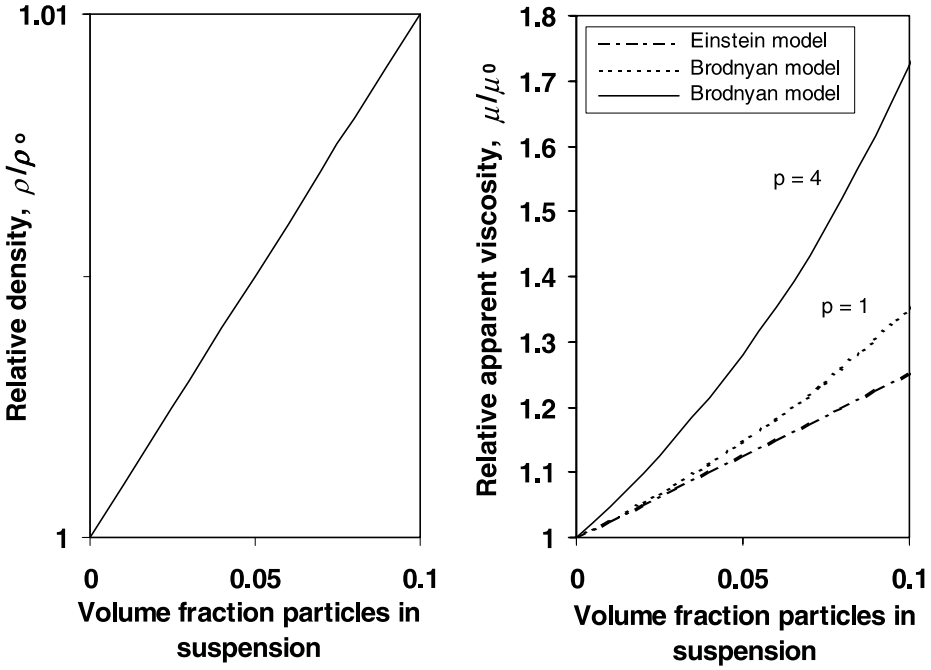

Fig. 6. Relative density and relative apparent viscosity as a function of the volume fraction of particles (bacterial cells) in suspension. The parameter p represents the ratio of the dimensions of the major and minor axis of an ellipsoidal particle.

stabilities arising from the density and viscosity variations that cannot be adequately resolved using continuum models. The same argument applies to variably saturated or unsaturated porous media systems, although the effects of density should be significantly less in unsaturated systems owing to the lack of buoyancy effects and the mitigating effects of capillarity.

Pore-scale instabilities may also be induced in variably saturated or multi-fluid systems by a microscopic phenomenon known as the Marangoni effect, which refers to the carrying of bulk material through motions energized by surface tension gradients [2]. Marangoni instabilities are often associated with temperature gradients that alter or create surface tension gradients [63]. However, such instabilities could also result from concentration gradients that might arise in variably saturated or multi-fluid systems due to solute displacement, substrate consumption, microbial growth, and/or biosurfactant production. Such instabilities could provide a potential mechanism for rapid spreading of surfactants across gas–liquid interfaces. This mechanism could result in desaturation of a variably saturated porous medium much more rapidly and extensively than would be predicted by standard continuum models of flow and transport.

7. Fluid-media scaling

In spite of the potential theoretical limitations noted above, the effects of changes in surface tension, contact angle, liquid density, and viscosity on the hydraulic properties of a variably saturated porous medium can be accounted for approximately in continuum flow and transport models by fluid-media scaling [49]. Changes in the air-entry pressure of a porous medium (see Eq. (12)) can be estimated by taking ratios of (11), which yields

$$h_{\mathrm{b}}^{*} = h_{\mathrm{b}}\left(\frac{\sigma}{\sigma_0}\right)\left(\frac{\rho_0}{\rho}\right)\beta \tag{21}$$

where h_{b}^{*} is a scaled air-entry pressure, σ and σ_0 are surface tensions at the gas–liquid interface, and ρ and ρ_0 are liquid densities, for the liquid-cell suspension and cell-free liquid (subscript 0), respectively, and β is a contact angle scaling factor. Surface tension and density can be measured as a function of bacterial cell concentrations, or estimated using Eqs. (18)–(20). Changes in surface tension due to biosurfactant production may be more difficult to quantify, however, since biosurfactant production will depend on several other factors in addition to cell concentration.

Taking ratios of (11) implies that the contact angle scaling factor $\beta = \cos\gamma/\cos\gamma_0$. This will be referred to as "simple" contact angle scaling. Using simple contact angle scaling in (21) is not strictly valid for non-zero contact angles because it violates the assumption of geometric similitude [49]. As noted previously, in subsurface environments it is typically assumed that porous media are water-wet so that the effective contact angle is constant and approximately equal to 0°. If this is the

case, then $\beta \approx 1$. However, if a porous medium becomes coated by biofilms, the assumption of a zero contact angle may no longer be appropriate because the biofilms may effectively change the wettability of the coated particle surfaces [1].

According to (9), at equilibrium, distinct contact angles can only occur at the point of contact between three separate phases—e.g. solid, liquid, and gas. This situation only occurs in porous media when the wetting fluid (usually water) is contained in discrete pendular rings that develop around the contact points between the solid particles (mineral grains), and when the rest of the particle surfaces are in direct contact with the non-wetting fluid (usually air) [22,48]. If the wettability of the particles is altered by biofilm formation, the determination of contact angle scaling factors for use in (21) may require an evaluation of the configuration of pendular water in the porous media.

Frankenfield and Selker [26] developed the following equations to describe surface area and volume relationships for a single pendular ring of liquid forming around the contact point between two equal-sized spherical particles

$$A_{ls} = 4\pi R^2(1-\cos\varphi) \tag{22}$$

$$A_{lg} = 4\pi R^2\left(\frac{1-\cos\varphi}{\sin\omega}\right)\{\omega[(1-\cos\varphi)\cot\omega + \sin\varphi] - (1-\cos\varphi)\} \tag{23}$$

$$V_p = 2\pi R^3\left\{(1-\cos\varphi)^2\left[1+\cot\omega\left[\sin\varphi+\cot\omega \times\left(1-\cos\varphi-\left(\frac{\sin\varphi}{\cos\omega}+\frac{1-\cos\varphi}{\sin\omega}\right)\frac{\omega}{\cos\omega}\right)\right]\right]\right\} \tag{24}$$

where A_{ls} and A_{lg} are the interfacial areas between the liquid and solid phases, and the liquid and gaseous phases, respectively, and where V_p is the volume of the pendular ring. The angle φ defines the size of the pendular ring and R is the radius of the solid particles (assumed uniform). A schematic of a pendular ring with relevant geometric terms is shown in Fig. 7. The term ω is defined by the size of the pendular ring and the contact angle as $\omega = \pi/2 - \varphi - \gamma$.

Frankenfield and Selker [26] used the following expression to relate changes in the surface energy of a pendular ring, ΔE_p, to changes in the interfacial areas and contact angle

$$\Delta E_p = \sigma_{lg}(\Delta A_{lg} + \Delta A_{ls}\cos\gamma) \tag{25}$$

The capillary pressure at a liquid–gas interface can be calculated by dividing the change in surface energy of a pendular ring by the change in its volume [41]

$$p_c = \frac{\Delta E_p}{\Delta V_p} \tag{26}$$

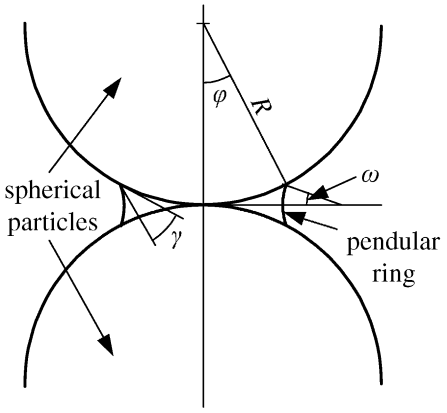

Fig. 7. Schematic diagram of a pendular ring of liquid around the contact between two spherical particles, with relevant geometric terms.

The liquid saturation corresponding to a given capillary pressure in a random packing of identical spherical particles can be calculated from the volume of a single pendular ring (given by 24) using equations from Gvirtzman and Roberts [27]. Noting that liquid saturation, S, is equal to the volumetric water content divided by porosity, these equations yield

$$S = \frac{3V_p}{8\phi\pi R^3}[26.49(1-\phi) - 10.73] \tag{27}$$

where ϕ is the porosity. Eqs. (22)–(27) can be used to calculate pressure–saturation relations for imbibition of any liquid into a dry porous medium consisting of uniform, spherical particles of size R, for any contact angle. Note, however, that these equations are only applicable for a finite range of values of the angle φ (see Fig. 7) such that individual pendular rings do not overlap with each other or with other particles.

Eqs. (22)–(27) are collectively referred to here and in Fig. 8 as the "FS" model. Fig. 8 shows pressure head–saturation relations calculated from the FS model for $\gamma = 0°$ and 30° for a 40/50 grade of Accusand® packed to a porosity of 0.33. The median grain diameter (d_{50}), uniformity coefficient (d_{60}/d_{10}), and particle sphericity for this sand are 0.359 ± 0.01 mm, 1.2 ± 0.018, and 0.9, respectively [65]. Also shown in Fig. 8 is a plot of the data representing values computed for $\gamma = 0°$ that have been scaled to $\gamma = 30°$ using (21) with simple contact angle scaling ($\beta = \cos\gamma/\cos\gamma_0$). The solution density and viscosity are assumed to be constant. As shown in Fig. 8, simple contact angle scaling results in the underestimation of the pressure head, relative to the FS model, for non-zero contact angles at all saturations.

New contact angle scaling factors, $\beta = P_c(\gamma)/P_c(0)$, were computed using the FS model and are plotted as a function of saturation (27) in Fig. 9. The solution density and viscosity were again assumed to be constant. Unlike simple contact angle scaling in which the scaling factors are only a function of the ratios of the cosines of

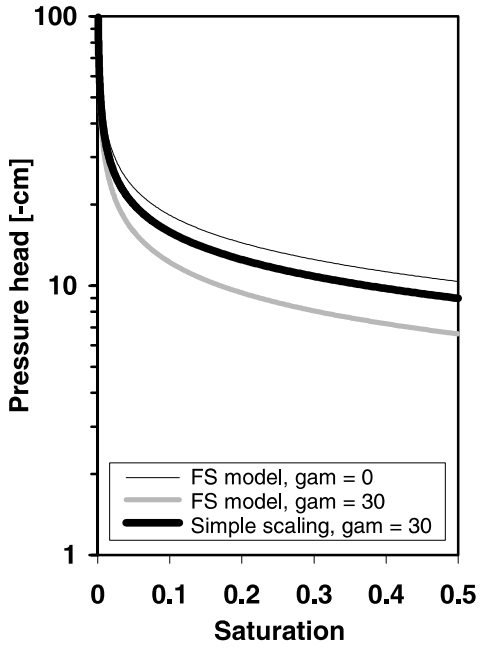

Fig. 8. Water retention curves calculated using the FS model corresponding to imbibition into dry porous media with contact angles, $\gamma = 0°$ and 30°. Also shown is a curve that is scaled from the results for $\gamma = 0°$ to $\gamma = 30°$ using simple contact angle scaling (see description in text).

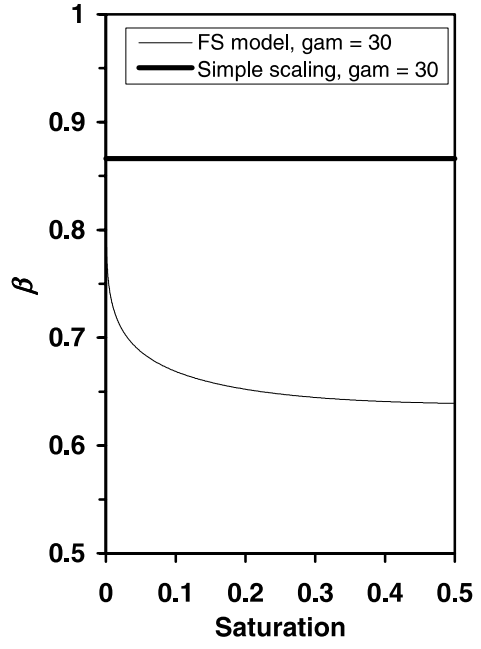

Fig. 9. Contact angle scaling factors, β, calculated as a function of wetting fluid saturation for $\gamma = 30°$ with the FS model and with simple contact angle scaling.

the contact angles, the scaling factors determined from the FS model are a function of both the contact angles and saturation. This is probably more realistic, but also makes the FS model more difficult to apply. Melrose [48] proposed a "curvature correction factor" to adjust the results obtained from simple contact angle scaling. Like simple contact angle scaling, the correction factor proposed by Melrose yields scaling factors that are independent of saturation. This correction factor results in smaller values of the scaling factors (or larger pressure corrections) relative to simple contact angle scaling. However, the scaling factors proposed by Melrose tend to overestimate pressure heads at low saturations, and underestimate pressure heads at higher saturations, relative to the FS model [26]. We assume that contact angle scaling based on the FS model is more accurate than either simple contact angle scaling or the method used by Melrose [48]. However, the applicability of the FS model has yet to be tested and may be limited by the fact that it relies on the assumption of uniform, spherical particles.

Accounting for changes in solution density, viscosity, and surface tension is relatively straightforward. However, the foregoing discussion suggests that accurately accounting for the effects of changes in contact angle is more complex. Additional difficulties arise when consideration is given to the various types of hysteresis that can also occur in the pressure–saturation–permeability relations for variably saturated porous media, and how biomass growth and accumulation might induce additional hysteretic phenomena. For the sake of brevity, the topic of hysteresis will not be discussed in detail here. Excellent papers on this topic can be found elsewhere [39,40,54].

It may be difficult to distinguish between changes in saturation that are due to changes in surface tension relative to those due to changes in contact angle. However, if the production of biosurfactants causes a lowering of surface tension, then this effect should be apparent locally, as well as downstream of the region in which the biosurfactant is being produced. On the other hand, if changes in saturation are due primarily to changes in contact angle resulting from attached biomass altering the wettability of the porous media, then this effect should be local to the area colonized by the bacteria.

Changes in the saturated hydraulic conductivity of a biomass-affected porous medium due to changes in solution density and viscosity can be estimated from

$$K_s^* = K_s \left(\frac{\mu_0}{\mu} \right) \left(\frac{\rho}{\rho_0} \right) \tag{28}$$

where K_s^* is the scaled value of the saturated hydraulic conductivity. Eq. (28) results from the definition of intrinsic permeability, $k = K_s \mu_0 / \rho_0 g$, by taking ratios of the solution viscosities and densities.

Eq. (28) is plotted as a function of the volume fraction of particles in suspension in Fig. 10, using the density and viscosity changes predicted by (18)–(20). Fig. 10a indicates that density and viscosity changes

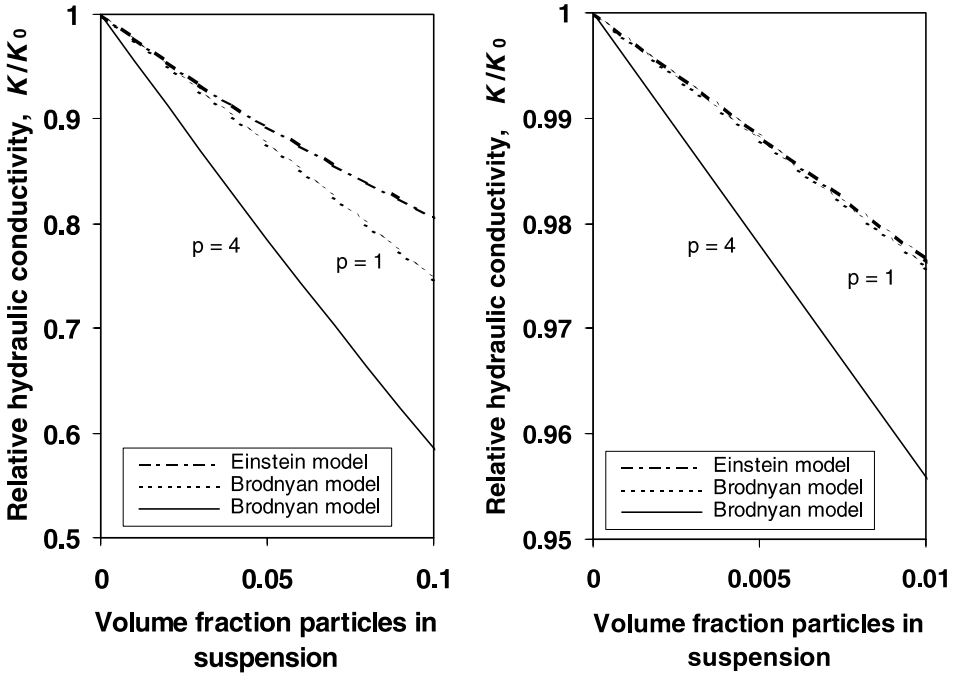

Fig. 10. Relative hydraulic conductivity as a function of volume fraction of particles (or bacterial cells) in suspension. The parameter p represents the ratio of the dimensions of the major and minor axis of an ellipsoidal particle.

caused by increases in aqueous-phase bacterial concentrations could potentially decrease hydraulic conductivity by 18–42% if the volume fraction of cells in suspension is 10%. Fig. 10b shows the potential changes in hydraulic conductivity due to density and viscosity over a smaller, and probably more realistic range of cell concentrations. Brodnyan's [10] model for ellipsoidal particles predicts a decrease in hydraulic conductivity of almost 4.5% resulting from density and viscosity increases corresponding to a volume fraction of 1% particles in solution. Changes in surface tension, contact angle, liquid density, and viscosity are all assumed to have no affect on the pore-size distribution index, λ, in (12).

8. Composite media model

Thus far we have only considered the possible effects of changes in the liquid-cell suspension and wettability on the effective hydraulic properties of variably saturated porous media. Accumulation of biomass attached to solid particles will also affect the hydraulic properties. As noted previously, several studies have observed bacterial cells that formed clusters or aggregates with void spaces that made up to an estimated 50% of their occupied volume [19–21]. The SEM photographs of Vandevivere and Baveye [76] also show the formation of porous bacterial aggregates (see Fig. 1). This type of infilling of the original pore space with a porous biomass phase could effectively lead to a composite porous media system with both primary and secondary porosity. Furthermore, data by Chenu [15] and others indicate that the EPS produced by some bacteria can have a tremendous water-holding capacity, which could also alter the hydraulic properties of a variably saturated porous medium.

A simple composite media model can be used to represent such systems. If the porous medium is sand, for example, the porosity of a composite porous medium consisting of the sand with a porous, attached biomass phase can be calculated from

$$\theta_s^{comp} = \theta_s^{sand} - n_f(1 - \theta_s^{bio}) \tag{29}$$

where n_f is defined by (5), and θ_s^{bio} is the assumed porosity of the attached biomass phase. An equation analogous to (29) has been used previously to estimate the porosity of sediment assemblages containing mixtures of sand and clay [34,46].

The volumetric liquid content of a composite porous medium whose porosity is given by (29) can be calculated as a function of pressure head, h, from

$$\theta_w^{comp}(h) = \theta_w^{sand}(h) - n_f\left\{\left[\frac{\theta_w^{sand}(h)}{\theta_s^{sand}}\right] - \theta_w^{bio}(h)\right\} \tag{30}$$

Eq. (30) implicitly assumes that the capillary pressure in the attached biomass phase is equal to that of the surrounding porous media. The hydraulic conductivity of the composite porous medium can be approximated by

$$K^{\mathrm{comp}}(\theta_{\mathrm{w}}^{\mathrm{comp}}) = K^{\mathrm{sand}}(\theta_{\mathrm{w}}^{\mathrm{sand}})\left[1 - \left(\frac{n_{\mathrm{f}}}{\theta_{\mathrm{s}}^{\mathrm{sand}}}\right)\right]^{b} + K^{\mathrm{bio}}(\theta_{\mathrm{w}}^{\mathrm{bio}})n_{\mathrm{f}} \tag{31}$$

where K^{sand} and K^{bio} are the hydraulic conductivities of the sand and the attached biomass phase, respectively, as a function of the volumetric water content of each phase, and b is an empirical parameter. If the attached biomass phase is assumed to be non-porous and impermeable, then $\theta_{\mathrm{s}}^{\mathrm{bio}}$ and K^{bio} would be equal to zero. For this case, if the b parameter is taken as equal to 19/6, and the porous medium is saturated, then (29) and (31) reduce to (6) and (3), respectively.

Eqs. (29)–(31) are applicable to variably saturated conditions. However, calculation of the liquid content (or saturation) and unsaturated hydraulic conductivity in this composite media model requires models for the liquid retention characteristics and hydraulic conductivities of both the original porous medium, as well as the attached biomass phase. Models such as those given by Brooks and Corey [11], van Genuchten [78], or others could be used for this purpose. Due to the fragility of microbial aggregates and biofilms, the independent determination of the parameters in these models would be difficult. Therefore, application of (29)–(31) would probably require that the parameters for the attached biomass phase be determined experimentally using observed liquid saturation and pressure data, combined with measurements of biovolume or attached biomass concentrations. However, non-destructive, in situ determination of biovolume or attached biomass concentrations is also extremely difficult. As an alternative, the saturated hydraulic conductivity of an attached biomass phase could be estimated from an assumed porosity and median cell size using the Kozeny–Carmen equation [7]. The water retention characteristics of an attached biomass phase could be estimated from the average cell density and an assumed cell-size distribution using a model such as that given by Arya and Paris [4]. Another alternative would be to simply assume that the hydraulic properties of the attached biomass phase are similar to a clay-textured soil.

Fig. 11 shows an example of the composite hydraulic properties of the 40/50 Accusand® containing different volume fractions of attached biomass (vfb), based on (29)–(31). van Genuchten [78] model is used in Fig. 11 to represent the attached biomass phase, with parameters that correspond to a clay-textured soil from Leij et al. [38]. The parameters used to represent the clay (or biomass) component with the van Genuchten [78] model are: $\theta_{\mathrm{s}} = 0.51$, $\theta_{\mathrm{r}} = 0.102$, $\alpha = 0.021\ \mathrm{cm}^{-1}$, $n = 1.2$, $K_{\mathrm{s}} = 1.08$ cm/h. The parameters used to represent the sand component with the Brooks and Corey [11] and Burdine [12] models are: $\theta_{\mathrm{s}} = 0.37$, $\theta_{\mathrm{r}} = 0.028$, $h_{\mathrm{b}} = 21.6$ cm, $\lambda = 5.84$, and $K_{\mathrm{s}} = 317$ cm/h.

The effects of the attached biomass become most apparent in the composite media model at relatively high biomass concentrations. Thus the use of such a model may be unnecessary in most cases, particularly in

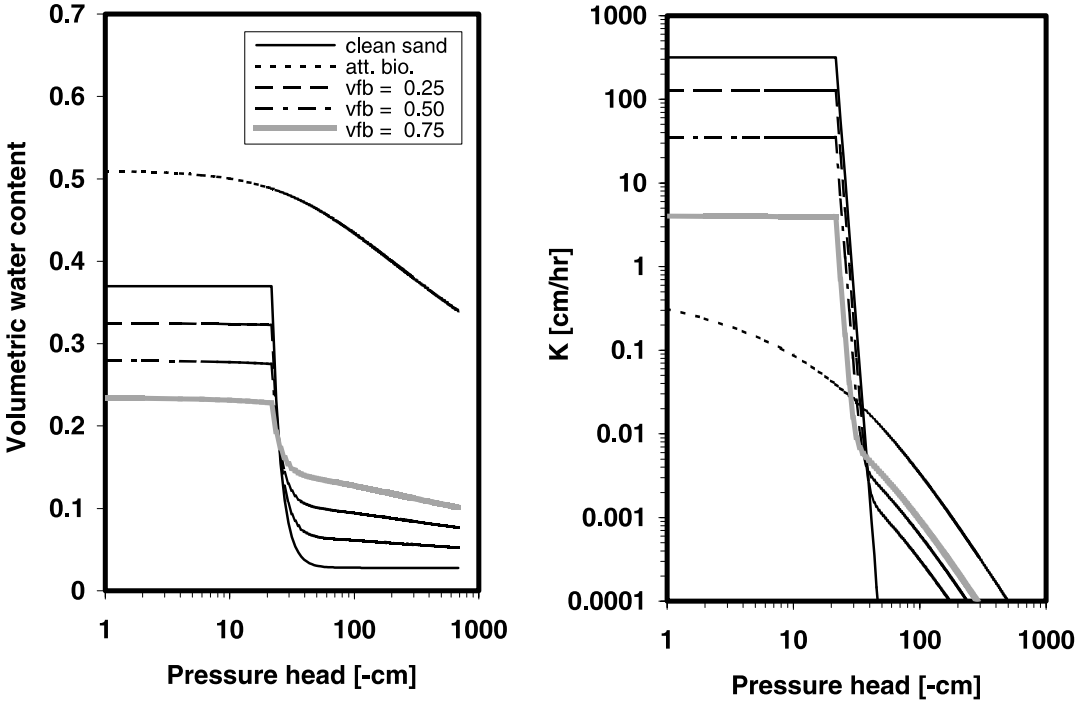

Fig. 11. Composite media model of volumetric water content and hydraulic conductivity as a function of pressure head for different vfb.

low nutrient environments. Nevertheless, Eqs. (29)–(31) provide a means of accounting for the possible effects of the accumulation of an attached biomass phase on the hydraulic properties of variably saturated porous media. Eqs. (29)–(31) can also be used in conjunction with (21) and (22) to simultaneously account for the effects of changes in surface tension, contact angle, solution viscosity and density, and infilling of the original pore space by a porous biomass phase. Note that a similar approach could also be applied in geochemical modeling to account for primary porosity reduction and secondary porosity formation and changes in hydraulic properties that might develop in variably saturated porous media during mineral precipitation/dissolution reactions.

The composite-media model given in (29)–(31) does not explicitly consider changes in the actual pore-size distribution of the porous media. An alternative to this model would be to discretize the water retention and hydraulic conductivity functions representing the clean porous media, and to account for biomass accumulation by explicitly changing the corresponding discretized form of the pore-size distribution. A hydraulic conductivity model such as that given by Childs and Collis-George [16] or others could be used in such a scheme to calculate relative permeability from a water retention function represented by piece-wise linear curve segments [62,68]. The water retention and hydraulic conductivity functions for the biomass-affected porous media could then be represented in numerical flow and transport models with tabular data, using table entries that are updated dynamically during a simulation. A potential problem with this approach would be deciding how to distribute the biomass within the water-filled pores. After this decision was made, however, the altered pore-size distribution could be readily used to recompute the water retention characteristics and hydraulic conductivity of the biomass-affected porous media. This approach might be more rigorous than the composite-media model, but it would also be more difficult to incorporate, and less efficient to use in numerical flow and transport models. From a practical perspective, considering the uncertainties associated with how biomass would actually be distributed within the pore space, the development and implementation of more rigorous approaches is probably unnecessary.

9. Summary and conclusions

Bacterial growth and accumulation in porous media systems is important in a variety of disciplines because it typically results in the reduction of the porosity and permeability of the porous media. The characteristics of the accumulated biomass are dependent on the type of bacteria, the substrate type and loading rate, surface and solution chemistries, and the flow rate. Several conceptual and mathematical models have been proposed for describing biomass-induced porosity and permeability reduction in saturated systems, with different assumptions about the morphology of the attached biomass phase. No universally applicable model has yet been developed for saturated porous media systems. Moreover, no attempts have been made prior to this one to develop or propose a model that is applicable to both saturated and unsaturated systems.

Unsaturated or variably saturated porous media are considerably more complicated than fully water-saturated systems, due to the fact that the water content and hydraulic conductivity are non-linear functions of capillary pressure rather than being constants as in saturated systems. Unsaturated systems are also complicated by the presence of gas–liquid interfaces. Previous studies have shown that preferential sorption of bacteria can occur at gas–liquid interfaces, relative to solid–liquid interfaces. This preferential sorption at gas–liquid interfaces has been attributed to bacterial cell surface hydrophobicity.

Sorption of cells at gas–liquid interfaces, and the production of surface-active compounds or biosurfactants during microbial metabolism, can result in lowering of surface tension and desaturation of variably saturated porous media. Desaturation tends to create more gas–liquid interfacial area that provides additional sites for sorption of bacterial cells and surfactants. Accumulation of cells and macromolecules at gas–liquid interfaces can also reduce the mass transfer rates of gases across gas–liquid interfaces. The solid–liquid contact angle, and hence the wettability of a porous medium may also change as it becomes coated by biofilms. These effects are unique to unsaturated porous media systems and may be important to consider for applications such as bioremediation, and for the design of septic and water treatment systems.

Additional changes that may be caused by the accumulation of bacterial cells in unsaturated or variably saturated porous media include increases in the viscosity and density of the bulk solution. Density effects should be much less significant in unsaturated porous media than in saturated porous media, however, due to the lack of buoyancy effects and the mitigating effects of capillarity. Gas generation and entrapment may also play a role in permeability reduction, in both saturated and unsaturated porous media, as bacteria metabolize substrates and generate carbon dioxide or other gases.

Very little effort has been made previously to address these issues for unsaturated porous media systems, from either a measurement or modeling perspective. Several simple expressions are discussed in this paper that can be used to model changes in the apparent viscosity and density of liquid-cell suspensions given the average cell

density and volume fraction of cells in suspension. These properties, as well as the apparent contact angle and surface tension as a function of cell and/or biosurfactant concentration can, in principle, be measured directly. Changes in these properties can be accounted for approximately in continuum models of flow and transport by scaling of the original constitutive relative permeability–saturation–capillary pressure relations for the porous media.

Accumulation of an attached biomass phase can also alter the pore structure of variably saturated porous media. A simple composite media model is presented that can be used to account for the accumulation of a porous attached biomass phase within the pore space. This composite-media model and the fluid-media scaling equations described herein can be readily incorporated into existing flow and transport models. It should be cautioned, however, that although biomass-induced changes in fluid-media properties of variably saturated porous media can be approximated in continuum flow and transport models using these methods, many of the potential changes that are described are due to microscopic phenomena and pore-scale instabilities that, depending on their magnitude, cannot always be represented accurately using continuum flow and transport models. These changes can also be expected to introduce additional non-linearities into the equations used for numerical modeling of water flow and reactive transport in variably saturated porous media.

In conclusion, bacterial-induced changes in the hydraulic properties of variably saturated porous media may be caused by many interacting factors, making the study of this topic very complicated. The study of these changes is further complicated by the fact that they cannot be easily observed in situ or non-destructively. This complexity probably explains the lack of prior research on this topic for unsaturated porous media. A series of subsequent papers will explore this topic further, presenting experimental observations of water content and pressure head changes, and concomitant changes in concentrations of substrate and bacteria during growth in a variably saturated sand. A numerical model is also under development that incorporates some of the equations described herein to model the coupled processes.

Acknowledgements

We would like to thank Fred Brockman for helpful discussions and Bruce Rittmann for providing valuable review comments. Financial support for this work was provided by the National Science Foundation (grant no. 9630293) and the Department of Energy (grant no. DE-FG07-98ER14925).

References

[1] Absolom DR, Lamberti FV, Policova Z, Zingg W, van Oss CJ, Neumann AW. Surface thermodynamics of bacterial adhesion. Appl Environ Microbiol 1983;46:90–7.
[2] Adamson AW, Gast AP. Physical chemistry of surfaces. New York: John Wiley and Sons; 1997.
[3] Alexander M. Biodegradation and bioremediation. San Diego, CA: Academic Press; 1994.
[4] Arya LM, Paris JF. A physicoempirical model to predict the soil moisture characteristic from particle size distribution and bulk density data. Soil Sci Soc Am J 1981;45:1023–30.
[5] Bailey JE, Ollis DF. Biochemical engineering fundamentals. New York: McGraw Hill; 1986.
[6] Baveye P, Valocchi A. An evaluation of mathematical models of the transport of biologically reacting solutes in saturated soils and aquifers. Water Resour Res 1989;25:1413–21.
[7] Bear J. Dynamics of fluids in porous media. New York: Dover Publications, Inc.; 1972.
[8] Beyenal H, Lewandowski Z. Mass-transport dynamics, activity, and structure of sulfate-reducing biofilms. Am Inst Chem Eng J 2001;47:1689–97.
[9] Bouwer EJ, Rittmann BE. Comment on: use of colloid filtration theory for modeling movement of bacteria through a contaminated sandy aquifer. Environ Sci Technol 1992;26:400–1.
[10] Brodnyan JG. The concentration dependence of the Newtonian viscosity of prolate ellipsoids. Trans Soc Rheol 1959;3:61–8.
[11] Brooks RH, Corey AT. Hydraulic properties of porous media. Hydrol Paper 3, Colorado State University, Fort Collins, 1964.
[12] Burdine NT. Relative permeability calculations from size distribution data. Trans Am Inst Mining Metal Petrol Eng 1953;198:71–7.
[13] Camesano TA, Logan BE. Influence of fluid velocity and cell concentration on the transport of motile and non-motile bacteria in porous media. Environ Sci Technol 1998;32:1699–708.
[14] Chahal RS. Effect of entrapped air and pressure on matric suction. Soil Sci 1966;102:131–4.
[15] Chenu C. Clay- or sand-polysaccharide associations as models for the interface between microorganisms and soil: water related properties and microstructure. Geoderma 1993;56:143–56.
[16] Childs EC, Collis-George N. The permeability of porous materials. Proc Roy Soc A 1950;201:392–405.
[17] Clement TP, Hooker BS, Skeen RS. Macroscopic models for predicting changes in saturated porous media properties caused by microbial growth. Ground Water 1996;34:934–42.
[18] Cunningham AB, Characklis WG, Abedeen F, Crawford D. Influence of biofilm accumulation on porous media hydrodynamics. Environ Sci Technol 1991;25:1305–11.
[19] De Beer D, Schramm A. Micro-environments and mass transfer phenomena in biofilms studied with micro-sensors. Water Sci Technol 1999;7:173–8.
[20] De Beer D, Stoodley P, Lewandowski Z. Liquid flow in heterogeneous biofilms. Biotechnol Bioeng 1994;44:636–41.
[21] De Beer D, Stoodley P, Roe F, Lewandowski Z. Effect of biofilm structures on oxygen distribution and mass transfer. Biotechnol Bioeng 1994;43:1131–8.
[22] Demond AH, Roberts PV. Effect of interfacial forces on two-phase capillary pressure–saturation relationships. Water Resour Res 1991;27:423–37.
[23] Déziel E, Paquette G, Villemur R, Lepine F, Bisaillon J. Biosurfactant production by a soil Pseudomonas strain growing on polycyclic aromatic hydrocarbons. Appl Environ Microbiol 1996;62:1908–12.
[24] Docoslis A, Giese RF, van Oss CJ. Influence of the water–air interface on the apparent surface tension of aqueous solutions of

hydrophilic solutes. Colloids Surf B: Biointerfaces 2000;19:147–62.
[25] Einstein A. The theory of brownian movement. New York: Dover Publishing, Inc; 1956 (English translation).
[26] Frankenfield J, Selker JS. Fluid interfacial geometry at the pore scale and its effect on characteristic curves. In: Proceedings of the 14th Annual Hydrology Days, Colorado State University, Fort Collins. Atherton, CO: Hydrology Days Publications; 1994. p. 111–22.
[27] Gvirtzman H, Roberts PV. Pore scale spatial analysis of two immiscible fluids in porous media. Water Resour Res 1991;27:1165–76.
[28] Hammel RK, Ratledge C. Biosynthetic mechanisms of low molecular weight surfactants and their precursor molecules. In: Kosaric N, editor. Biosurfactants. New York: Marcel Dekker, Inc.; 1993. p. 3–63.
[29] Happel J, Brenner H. Low Reynolds number hydrodynamics. Englewood Cliffs, NJ: Prentice Hall; 1965.
[30] Heath MS, Wirtel SA, Rittmann BE. Simplified design of biofilm processes using normalized loading curves. Res J Water Pollut Control Fed 1990;62:185–92.
[31] Heath MS, Wirtel SA, Rittmann BE, Noguera DR. Closure to simplified design of biofilm processes using normalized loading curves. Res J Water Pollut Control Fed 1991;63:91–2.
[32] Istok JD, Humphrey MD. Laboratory investigation of buoyancy-induced flow (plume sinking) during two-well tracer tests. Ground Water 1995;33:597–604.
[33] Jenneman GE, Knapp RM, McInerney MJ, Menzie DE, Revus DE. Experimental studies of in situ microbial enhanced oil recovery. Soc Petrol Eng J 1984;24:33–7.
[34] Kolterman CE, Gorelick SM. Fractional packing model for hydraulic conductivity derived from sediment mixtures. Water Resour Res 1995;31:3283–97.
[35] Kosaric N, editor. Biosurfactants. New York: Marcel Dekker, Inc.; 1993.
[36] Lawrence JR, Delaquis PJ, Korber DR, Caldwell DE. Behavior of *Pseudomonas fluorescens* within the hydrodynamic boundary layers of surface microenvironments. Microbiol Ecol 1987;14:1–14.
[37] Leffelaar PA. Dynamics of partial anaerobiosis, denitrification, and water in a soil aggregate: simulation. Soil Sci 1988;146:427–44.
[38] Leij FJ, Alves WJ, van Genuchten MTh. The UNSODA unsaturated soil hydraulic database characterization and measurement of the hydraulic properties of unsaturated porous media, Part 2. In: van Genuchten MTh, Leij FJ, Wu L, editors Riverside, CA: University of California Press; 1999. p. 1269–81.
[39] Lenhard RJ, Parker JC. A model for hysteretic constitutive relations governing multiphase flow. 2. Permeability-saturation relations. Water Resour Res 1987;23:2197–206.
[40] Lenhard RJ, Parker JC, Kaluarachchi JJ. A model for hysteretic constitutive relations governing multiphase flow. 3. Refinements and numerical simulations. Water Resour Res 1989;25:1727–36.
[41] Leverett MC. Capillary behavior in porous solids. Trans Am Inst Mining Metal Petrol Eng 1941;142:152–69.
[42] Lewandowski Z. Structure and function of biofilms biofilms: recent advances in their study and control. In: Evans LV, editor New York: Harwood Academic Publishers; 2000. p. 1–17.
[43] Lewandowski Z, Webb D, Hamilton M, Harkin G. Quantifying biofilm structure. Water Sci Technol 1999;39:71–6.
[44] MacDonald TR, Kitanidis PK, McCarty PL, Roberts PV. Mass-transfer limitations for macroscale bioremediation modeling and implications on aquifer clogging. Ground Water 1999a;4:523–31.
[45] MacDonald TR, Kitanidis PK, McCarty PL, Roberts PV. Effects of shear detachment on biomass growth and in situ bioremediation. Ground Water 1999b;4:555–63.
[46] Marion D, Nur A, Yin H, Han D. Compressional velocity and porosity in sand–clay mixtures. Geophys 1992;57:554–63.
[47] Marshall KC. Adsorption and adhesion processes in microbial growth at interfaces. In: Advances in colloid and interface science, vol 25. Amsterdam: Elsevier Science Publishers; 1986. p. 59–86.
[48] Melrose JC. Wettability as related to capillary action in porous media. Soc Petrol Eng J 1965;5:259–71.
[49] Miller EE, Miller RD. Physical theory for capillary flow phenomena. J Appl Phys 1956;27:324–32.
[50] Molz FJ, Widdowson MA, Benefield LD. Simulation of microbial growth dynamics coupled to nutrient and oxygen transport in porous media. Water Resour Res 1986;22:1207–16.
[51] Mualem Y. A new model for predicting the hydraulic conductivity of unsaturated porous media. Water Resour Res 1976;12:513–22.
[52] Murphy EM, Ginn TR, Chilakapati A, Resch CT, Phillips JL, Wietsma TW, et al. The influence of physical heterogeneity on microbial degradation and distribution in porous media. Water Resour Res 1997;33:1087–103.
[53] Ouyang Y, Zheng C. Density-driven transport of dissolved chemicals through unsaturated soil. Soil Sci 1999;164:376–90.
[54] Parker JC, Lenhard RJ. A model for hysteretic constitutive relations governing multiphase flow. 1. Saturation–pressure relations. Water Resour Res 1987;23:2187–96.
[55] Raiders RA, McInerney MJ, Revus DE, Torbati HM, Knapp RM, Jenneman GE. Selectivity and depth of microbial plugging in Berea sandstone cores. J Indust Microbiol 1986;1:195–203.
[56] Rittmann BE. The effect of shear stress on biofilms loss rate. Biotechnol Bioeng 1982;24:501–6.
[57] Rittmann BE. Analyzing biofilm processes used in biological filtration. J Am Water Works Assoc 1990;82:62–6.
[58] Rittmann BE. The significance of biofilms in porous media. Water Resour Res 1993;29:2195–202.
[59] Rittmann BE, McCarty PL. Model of steady-state biofilm kinetics. Biotechnol Bioeng 1980a;22:2343–57.
[60] Rittmann BE, McCarty PL. Evaluation of steady-state biofilm kinetics. Biotechnol Bioeng 1980b;22:2359–73.
[61] Roberson EM, Firestone MK. Relationship between dessication and exopolysaccharide production in a soil *Pseudomonas* sp. Appl Environ Microbiol 1992;58:1284–91.
[62] Rockhold ML, Simmons CS, Fayer MJ. An analytical solution technique for one-dimensional, steady vertical water flow in layered soils. Water Resour Res 1997;33:897–902.
[63] Ruckenstein E, Suciu DG, Smigelschi O. Spreading on liquids: effect of surface tension sinks on the behavior of stagnant liquid layers. In: Schrader ME, Loeb GI, editors. Modern approaches to wettability theory and applications. New York: Plenum Press; 1992. p. 397–422.
[64] Schäfer A, Ustohal P, Harms H, Stauffer F, Dracos T, Zehnder AJB. Transport of bacteria in unsaturated porous media. J Contam Hydrol 1998;33:149–69.
[65] Schroth MH, Ahern SJ, Selker JS, Istok JD. Characterization of Miller-similar silica sands for laboratory hydrologic studies. Soil Sci Soc Am J 1996;60:1331–9.
[66] Schügerl K. Characterization and performance of single- and multistage tower reactors with outer loop for cell mass production. In: Fiechter A, editor. Advances in biochemical engineering, vol 22A. New York: Springer-Verlag; 1982. p. 94–217.
[67] Seki K, Miyazaki T, Nakano M. Effects of microorganisms on hydraulic conductivity decrease in infiltration. Eur J Soil Sci 1998;49:231–6.
[68] Simmons CS, Lenhard RJ, Demond AH. A general analytical model for three phase immiscible fluid relative permeability. EOS Abstracts, Annual Fall meeting of the American Geophysical Union, San Francisco, CA, 1991.
[69] Speitel GE, DiGiano FA. Biofilm shearing under dynamic conditions. J Environ Eng 1987;113:464–75.

[70] Taylor SW, Jaffe PR. Biofilm growth and the related changes in the physical properties of a porous medium. 1. Experimental investigation. Water Resour Res 1990a;26:2153–9.
[71] Taylor SW, Jaffe PR. Biofilm growth and the related changes in the physical properties of a porous medium. 3. Dispersivity and model verification. Water Resour Res 1990b;26:2171–80.
[72] Taylor SW, Jaffe PR. Substrate and biomass transport in a porous medium. Water Resour Res 1990c;26:2181–94.
[73] Taylor SW, Milly PCD, Jaffe PR. Biofilm growth and related changes in the physical properties of a porous medium, 2. Permeability. Water Resour Res 1990;26:2161–9.
[74] Vandevivere P. Bacterial clogging of porous media: a new modeling approach. Biofouling 1995;8:281–91.
[75] Vandevivere P, Baveye P. Relationship between transport of bacteria and their clogging efficiency in sand columns. Appl Environ Microbiol 1992a;58:2523–30.
[76] Vandevivere P, Baveye P. Saturated hydraulic conductivity reduction caused by aerobic bacteria in sand columns. Soil Sci Soc Am J 1992b;56:1–13.
[77] Vandevivere P, Kirchman DL. Attachment stimulates exopolysaccharide synthesis by a bacterium. Appl Environ Microbiol 1993;59:3280–6.
[78] Van Genuchten MTh. A closed-form equation for predicting the hydraulic conductivity of unsaturated soils. Soil Sci Soc Am J 1980;44:892–8.
[79] Van Genuchten MTh., Leij FJ, Yates SR. The RETC code for quantifying the hydraulic functions of unsaturated soils, US Environmental Protection Agency, Robert S. Kerr Environmental Research Laboratory, Ada, Oklahoma, EPA/600/2-91/065, 1991.
[80] Wan J, Wilson JL. Colloid transport in unsaturated porous media. Water Resour Res 1994;30:857–64.
[81] Wan J, Wilson JL, Kieft TL. Influence of the gas-water interface on transport of microorganisms through unsaturated porous media. Appl Envir Microbiol 1994;60:509–16.
[82] Wirtel SA, Noguera DR, Kampmeier DT, Heath MS, Rittmann BE. Explaining widely varying biofilm-process performance with normalized loading curves. Water Environ Res 1992;64:706–11.
[83] Widdowson MA. Comment on: An evaluation of mathematical models of the transport of biologically reacting solutes in saturated soils and aquifers. Water Resour Res 1991;27:1375–8.
[84] Widdowson MA, Molz FJ, Benefield LD. A numerical transport model for oxygen- and nitrate-based respiration linked to substrate and nutrient availability in porous media. Water Resour Res 1988;24:1553–65.
[85] Yang X, Beyenal H, Harkin G, Lewandowski Z. Quantifying biofilms structure using image analysis. J Microbiol Meth 2000;39:109–19.